

# Inactivation pathways of *Escherichia coli* and *Staphylococcus aureus* induced by transient spark discharge in liquids

Aleksandra Lavrikova<sup>1</sup>  | Nitin Chandra Teja Dadi<sup>2</sup> | Helena Bujdaková<sup>2</sup>  | Karol Hensel<sup>1</sup> 

<sup>1</sup>Division of Environmental Physics, Faculty of Mathematics, Physics and Informatics, Comenius University, Bratislava, Slovakia

<sup>2</sup>Department of Microbiology and Virology, Faculty of Natural Sciences, Comenius University, Bratislava, Slovakia

## Correspondence

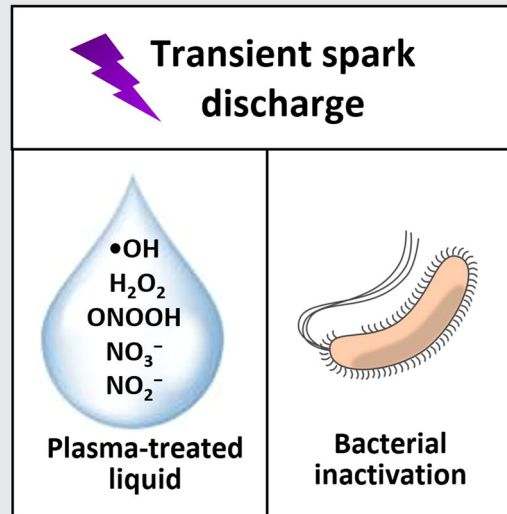
Karol Hensel, Division of Environmental Physics, Faculty of Mathematics, Physics and Informatics, Comenius University, 842 48 Bratislava, Slovakia.  
Email: [hensel@fmph.uniba.sk](mailto:hensel@fmph.uniba.sk)

## Funding information

Slovak Research and Development Agency, Grant/Award Numbers: APVV-20-0566, APVV-22-0247; Slovak Grant Agency, Grant/Award Number: VEGA 1/0596/22; "PlasTHER" COST Action (European Cooperation in Science and Technology), Grant/Award Number: CA20114

## Abstract

Cold plasma finds considerable interest in biodecontamination. A major issue is to elucidate the pathways of plasma–bacteria interaction. The present work aims at studying inactivation mechanisms for planktonic bacteria *Escherichia coli* and *Staphylococcus aureus* induced by cold plasma generated by a transient spark discharge. Changes in bacterial viability, metabolic activity, membrane integrity, intracellular reactive oxygen species level, and cell morphology reveal different patterns of cellular damage of the bacteria. Our results emphasize the importance of cell membrane integrity and maintenance of intracellular redox balance to resist plasma treatment. The physicochemical properties of the plasma-treated liquid (PTL) are monitored. Acidification and accumulation of various reactive species including  $\bullet\text{OH}$ ,  $\text{H}_2\text{O}_2$ ,  $\text{ONOOH}$ , and  $\text{NO}_3^-$  in PTL play crucial roles in bacterial inactivation.



## KEYWORDS

bactericidal effects, cold plasma, *Escherichia coli*, plasma-treated liquids, *Staphylococcus aureus*, transient spark

## 1 | INTRODUCTION

Microbial inactivation is one of the biggest issues for medicine, the food industry, agriculture, and environmental protection. Conventional decontamination methods, such

as heat treatments, high-pressure processing, ultraviolet (UV) radiation, photochemical oxidation, pulsed electric field, ozonation, fumigation, filtration, chemical disinfectants (formaldehyde, chlorine, hydrogen peroxide [ $\text{H}_2\text{O}_2$ ], alkylammonium salts, etc.), have the potential to reduce

pathogenic microorganisms. However, hazardous chemical residues, thermal damages, and insufficient antimicrobial effect challenge their safe utilization. Besides, the problem of antibiotic resistance poses the biggest threat to global health nowadays. It is largely linked to antibiotic misuse and overuse, as well as a wide spread of antibiotic-resistant pathogens in aquatic environments, that is, surface and groundwater, sewage treatment plants, aquaculture farms, and so forth.<sup>[1]</sup> There is an extreme necessity for new effective and affordable biodecontamination and sterilization methods.

Cold atmospheric pressure plasma represents an easy and environmentally friendly method. It refers to nonequilibrium ionized quasineutral gas composed of charged and neutral species, free radicals, electromagnetic fields, and UV radiation. The plasma has exhibited great potential for microbial decontamination and has been effectively tested in bactericidal, virucidal, sporicidal, and antiparasite activity.<sup>[2]</sup> Moreover, liquids treated by the plasma (e.g., water, phosphate-buffered saline [PBS], culture media), referred to as plasma-treated liquids (PTLs), possess various biological effects given by the concentration of reactive oxygen and nitrogen species (RONS) in the liquids.<sup>[3]</sup> Indirect plasma treatment mediated by PTLs has attracted special attention due to their competitiveness to direct plasma treatment effects. It has demonstrated antimicrobial, anticancer, wound healing, and other interesting effects.<sup>[4]</sup> Therefore, plasma-liquid and plasma-cell interactions in aqueous solutions are being explicitly studied in the past two decades owing to multiple promising plasma applications.

It is obvious that adaptation of the plasma technology for biodecontamination is plausible. Although the antibacterial activity of the plasma is indisputably confirmed in diverse applications, the plasma-bacteria interaction pathways and mechanisms of plasma-induced bacterial inactivation are yet to be fully explored. It is generally agreed that the effect of plasma on bacterial cells is related to the interaction of plasma reactive species (RONS) with cell components leading to a combination of biophysical attack (morphological destruction) and biochemical pathways (lipid peroxidation, DNA degradation, protein dysfunctioning).<sup>[5]</sup> Bacteria may confer different resistance to plasma treatment. The bacterial cell membrane structure is the major factor of susceptibility to multicomponent plasma attack. Plasma-generated species can react with both lipopolysaccharide (LPS) and peptidoglycan breaking the molecular structure by damaging C–O, C–N, and C–C bonds.<sup>[6]</sup> However, peptidoglycan is less susceptible to chemical oxidation than LPS.<sup>[7]</sup> Therefore, the thin peptidoglycan layer (~2 nm) of Gram-negative (Gram<sup>-</sup>) bacteria defines a more vulnerable cellular envelope in

contrast to Gram-positive (Gram<sup>+</sup>) bacteria with a thicker peptidoglycan layer (~15–18 nm). It is easier to achieve the disruption of membrane integrity of Gram<sup>-</sup> bacteria while Gram<sup>+</sup> ones are more likely to undergo intracellular oxidative reactions with insignificant envelope damage.<sup>[8,9]</sup> Naturally produced ROS during the respiratory electron transport chain are maintained at low levels by the cellular antioxidant defense system. When the balance of intracellular ROS is disturbed, bacteria can intensify endogenous ROS production or lose the ability to detoxify or repair. Thus, non-scavenged ROS overwhelm the defense system and dramatically injure cells.<sup>[10]</sup> Biological targets for RONS in a microbial cell include thiols, metal centers, protein tyrosins, nucleotide bases, and lipids.<sup>[11]</sup> For instance, •OH is the most harmful species that reacts at a diffusion-controlled rate with all biomolecules,<sup>[12]</sup> ONOO<sup>-</sup> and H<sub>2</sub>O<sub>2</sub> react with proteins, lipids, and DNA, and cause their oxidation, HO<sub>2</sub> may be an initiator of lipid peroxidation, <sup>1</sup>O<sub>2</sub> causes cell death, NO can be bactericidal directly or by conversion to ONOO<sup>-</sup>.<sup>[13]</sup> <sup>1</sup>O<sub>2</sub> and H<sub>2</sub>O<sub>2</sub> were found to be a cause of membrane lipid peroxidation and oxidative DNA damage of *Escherichia coli*, leading to rapid bacterial inactivation by a dielectric barrier discharge (DBD).<sup>[14]</sup> Atomic O, •OH, and O<sub>3</sub> were reported to suppress bacterial metabolic activity and cause physical destruction of *E. coli* and *Bacillus subtilis* treated by pulsed DBD.<sup>[15]</sup> ONOO<sup>-</sup> was identified as the main oxidative killing species of *E. coli* treated by air plasma jet<sup>[16]</sup> and corona discharge (O<sub>2</sub>, N<sub>2</sub>, and air),<sup>[17]</sup> as well as transient spark (TS) discharge (N<sub>2</sub>/O<sub>2</sub> mixtures).<sup>[18]</sup> High concentrations of Cl<sup>-</sup> ions in PTLs (PBS, NaCl, culture media) may cause the generation of cytotoxic chlorine compounds (HOCl, OCl<sup>-</sup>, ClO<sub>2</sub>, ClO<sub>3</sub>, NaOCl, NH<sub>2</sub>Cl) following the reactions of RONS with Cl<sup>-</sup>.<sup>[19]</sup> It was shown that the presence of NaCl in solution led to the formation of long-lived species (ClO<sup>-</sup>), which played the main role in inactivation. ClO<sup>-</sup> is dominantly generated via the reactions with O, mainly in plasmas that generate a high amount of O atoms and a limited amount of peroxides and oxidized nitrogen species.<sup>[19,20]</sup> The presence of H<sub>2</sub>O<sub>2</sub> and NO<sub>2</sub><sup>-</sup> leads rather to fast consumption of generated ClO<sup>-</sup>.<sup>[20]</sup>

The present study contributes relevant knowledge to an elucidation of the complex plasma-bacteria interaction pathways. Many existing studies usually deal with one type of bacteria, in one growth phase, and the effect of plasma is evaluated by a limited number of experimental techniques. The comprehensive analysis of plasma effects on Gram<sup>-</sup> *E. coli* and Gram<sup>+</sup> *Staphylococcus aureus* in different growth phases confronted with chemical characterization of PTL emphasizes the originality of our research. The unique configuration of the

TS discharge allowed the circulation of a thin stream of a liquid sample through the discharge plasma zone. It is an efficient way to increase the plasma–liquid interaction and transfer of gas-phase species into PTL. In the present work, for the first time, such a “dynamic” plasma system was examined for biodecontamination of two planktonic bacteria *E. coli* and *S. aureus* in saline with an emphasis on detailed inactivation mechanisms. Significant inactivation of *E. coli* induced by TS discharge was shown in our previous studies. Higher inactivation was found for bacteria suspended in nonbuffered (3–5 log) than in buffered (1–2 log) water solutions.<sup>[21]</sup> Later, the gas composition was shown to affect *E. coli* inactivation in nonbuffered monosodium phosphate  $\text{NaH}_2\text{PO}_4 \cdot 2\text{H}_2\text{O}$  solution. The TS discharge generated in pure  $\text{O}_2$ ,  $\text{N}_2$ , and  $\text{O}_2 + \text{N}_2$  caused 2 log, 2.5 log, and 3.6 log reductions, respectively.<sup>[18]</sup> Here, the plasma-induced damages of *E. coli* and *S. aureus* and the roles of different RONS during plasma treatment were determined. Bacterial viability, metabolic activity, cell membrane integrity, accumulation of intracellular ROS, and morphology were investigated. The physicochemical properties of PTL, including pH, conductivity, oxidation–reduction potential (ORP),

and concentration of long-lived ( $\text{H}_2\text{O}_2$ ,  $\text{NO}_2^-$ ,  $\text{NO}_3^-$ ) and accumulated total amount of short-lived ( $\cdot\text{OH}$ ,  $\text{ONOO}^-$ ) reactive species were monitored. Based on the physicochemical properties of the PTL, we reported potential patterns of plasma inactivation mechanisms on essential nosocomial pathogens *E. coli* and *S. aureus*.

## 2 | EXPERIMENTAL SETUP AND METHODS

### 2.1 | TS discharge

Transient spark (TS) discharge is a direct current (DC)-driven self-pulsing repetitive streamer to spark transition discharge generated in atmospheric pressure. TS generates highly reactive nonequilibrium filamentary plasma discharge thanks to the spark pulses of short duration (~10–100 ns), high amplitude (10–100 A), and high repetition rate (1–10 kHz). Figure 1 shows the experimental setup and characteristic discharge voltage and current waveforms.

The setup consists of point-to-plane electrode configuration with an high voltage (HV) needle electrode

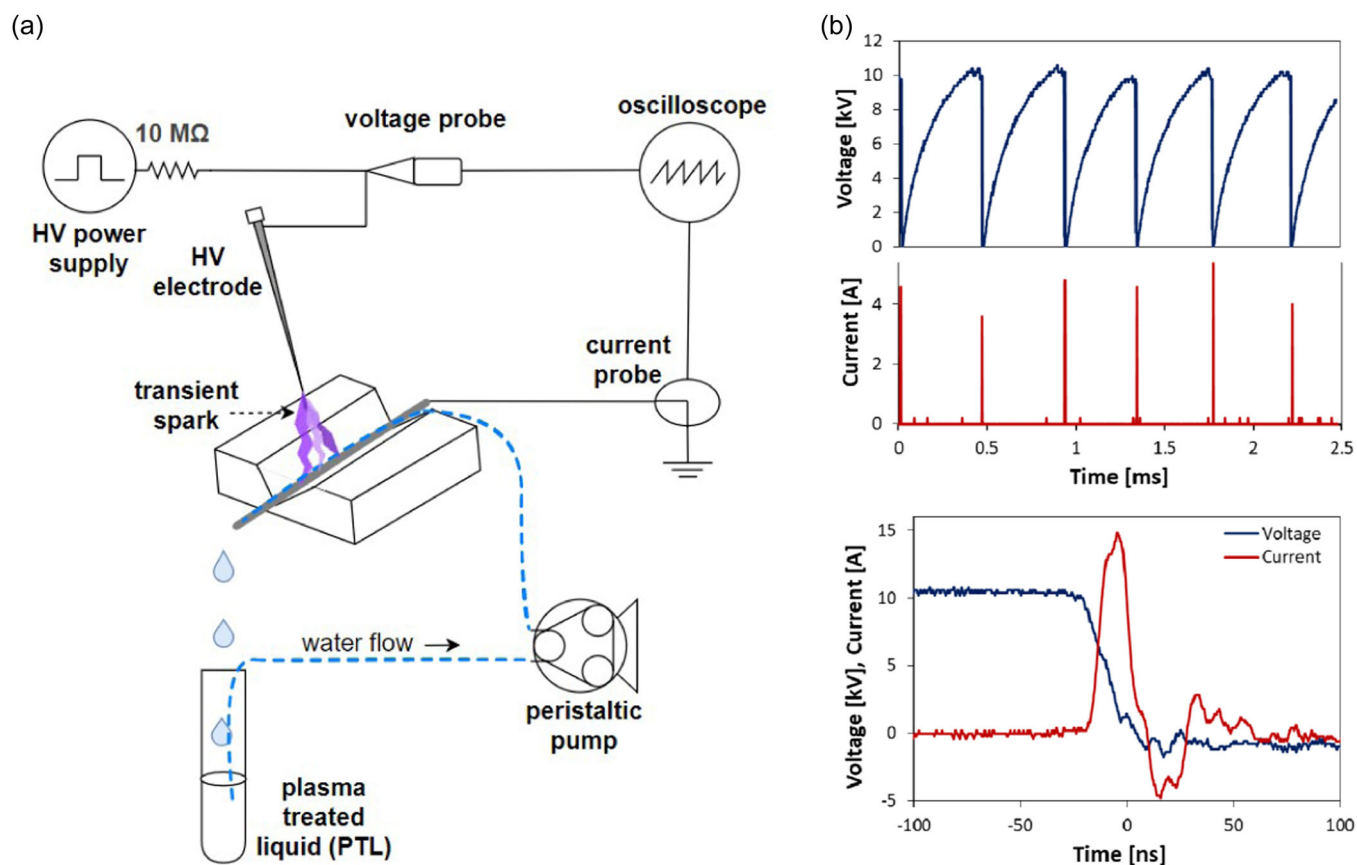


FIGURE 1 (a) Scheme of the experimental setup and (b) characteristic voltage and current waveforms of a transient spark discharge in two different timescales.

placed against a grounded plane electrode embedded inside a narrow polytetrafluoroethylene channel inclined at an angle of 45° to let liquid move down the electrode. The distance between the electrodes was ~1 cm. The liquid was driven via a narrow channel and circulated by a peristaltic pump (Masterflex L/S) with a constant flow rate of 14 mL/min to provide for repetitive contact with the discharge. The TS discharge was driven by a positive DC HV power supply (CX-300B) and its electrical characteristics were monitored by the HV probe (Tektronix P6015A) and Rogowski-type current probe (Pearson Electronics 2877) connected to a digitizing oscilloscope (Tektronix TBS 2000). Positive DC HV was applied through the ballast resistor R (10 MΩ) to maintain the TS discharge mode operating in the following typical conditions: generator voltage ~14–16 kV, current peak amplitude ~10–20 mA, and current pulse repetition rate ~2 kHz. A detailed description of the TS discharge, and its electrical and optical characteristics, have been published in our previous works.<sup>[22,23]</sup> In this study, TS discharge was used for the treatment of saline for the identification of plasma-generated RONS and bacterial suspensions in saline for bactericidal effects.

## 2.2 | PTL characterization

Sterile saline solution (0.85% NaCl in deionized [DI] water [DW], pH 6.5) was used in experiments to generate PTL. The temperature and pH were measured by pH probe (WTW pH-electrode SenTix 60), electrical conductivity by the conductivity meter (Greisinger Electronic GMH 3430), and ORP by ORP probe (WTW SenTix ORP 103648). The chemical composition of PTL was measured by well-established UV/visible (Shimadzu UV-1900) and fluorescence (Shimadzu RF-6000) spectrophotometric methods. H<sub>2</sub>O<sub>2</sub> was detected by its reaction with titanil ions Ti<sup>4+</sup> of titanium oxysulfate (TiOSO<sub>4</sub>) resulting in a yellow-colored product of pertitanic acid (H<sub>2</sub>TiO<sub>4</sub>) with an absorbance maximum at 407 nm.<sup>[24]</sup> The nitrite NO<sub>2</sub><sup>-</sup> concentration was measured by Griess reagents (Cayman Chemicals) under acidic conditions resulting in a pink-colored azo-product with an absorbance maximum at 540 nm.<sup>[25]</sup> The nitrate NO<sub>3</sub><sup>-</sup> concentration was measured by a combined nitrate selective electrode (WTW NO 800 DIN). Since the lifetime of •OH and ONOO<sup>-</sup> is in the nanosecond scale,<sup>[26]</sup> their steady-state concentration cannot be measured after the discharge as in the case of species above (H<sub>2</sub>O<sub>2</sub>, NO<sub>2</sub><sup>-</sup>, NO<sub>3</sub><sup>-</sup>). Instead, their concentration was measured indirectly by using chemical probes present in a saline solution before the plasma treatment. However, in such a case, the evaluated concentration represents the total amount of accumulated radicals, not

their steady-state concentration. The hydroxyl radical •OH concentration was measured by chemical dosimetry using terephthalic acid,<sup>[27]</sup> resulting in 2-hydroxyterephthalic acid (HTA) detected by fluorescence spectrometry with excitation and emission wavelengths 310 and 425 nm, respectively.<sup>[28]</sup> The peroxyxynitrite (ONOO<sup>-</sup>) concentration was measured by a fluorometric assay kit (Abcam; ab233469), resulting in a bright green fluorescent product measured at excitation and emission wavelengths 490 and 530 nm, respectively. The chlorine (Cl<sup>-</sup>) concentration was measured by a combined chloride electrode (Fisher Scientific). The hypochlorite (ClO<sup>-</sup>) concentration was measured spectrophotometrically at its absorption maximum of 292 nm.<sup>[19]</sup>

## 2.3 | Bacterial cultures and sample preparation

Bactericidal effects were tested on standard strains of Gram<sup>-</sup> *E. coli* CCM3954 and Gram<sup>+</sup> *S. aureus* CCM3953 from the Czech Collection of Microorganisms. Bacteria were grown on Luria–Bertani (LB) agar (Biolab). Isolated colonies were inoculated into LB broth and incubated overnight (18 h) at 37°C with shaking by multispeed vortex (Biosan MSV-3500) at 300 rpm. The bacterial suspensions from overnight cultures corresponded to the stationary (*stat*) phase of growth. Then, the suspensions were inoculated in fresh LB broth to obtain an OD<sub>600</sub> (optical density at λ = 600 nm) of 0.05 (~10<sup>7</sup> CFU/mL) and cultivated at 37°C with shaking as described above. The exponential (*exp*) phase (OD<sub>600</sub> ≈ 0.5) was determined to be after 2.5–3.5 h incubation. Inocula prepared from *stat* and *exp* phase of growth were harvested by centrifugation (Hettich Universal 320) for 10 min at 8000 rpm. The bacterial cell pellets were washed twice with saline and then resuspended in saline to obtain the required initial concentration of 1 × 10<sup>7</sup> CFU/mL for treatment.

Planktonic bacteria in 5 mL saline solution in 15-mL tubes were directly exposed to TS discharge for a given time of 5, 10, 15, and 20 min. Then, each suspension was centrifuged at 8000 rpm for 5 min, and the supernatant was replaced with fresh saline to avoid a postplasma delayed effect. For each type of bacterial analysis, the plasma treatment was carried out separately.

## 2.4 | Bacterial viability

The viability of bacteria after plasma treatment was estimated by the colony count assay and compared with the untreated control. Briefly, several 10-fold dilution

series (a 100  $\mu\text{L}$  sample mixed with 900  $\mu\text{L}$  saline) were performed, spread on LB agar plates, and colonies were enumerated for viable cells as colony-forming units (CFUs) after 24 h of incubation at 37°C. The bactericidal effect of each treatment was expressed in terms of log reduction,  $\log(N_0/N)$ , where  $N_0$  and  $N$  are the numbers of viable cells before and after treatment, respectively.

## 2.5 | Bacterial metabolic activity

The colorimetric tetrazolium dye 3-(4,5-di-methylthiazol-2-yl)-2,5-diphenyltetrazolium bromide (MTT) assay was used for evaluating the metabolic activity of bacteria. NAD(P)H-dependent cellular oxidoreductase enzymes reduce the MTT (Sigma-Aldrich) at a concentration of 0.5 mg/mL in PBS (Sigma-Aldrich) to its insoluble formazan, which has a purple color.<sup>[29]</sup> The assay was carried out in 96-well microtiter plates by mixing 90  $\mu\text{L}$  of the sample with 10  $\mu\text{L}$  of the MTT solution following incubation in the dark for 30 min at 37°C with gentle shaking. Then, 100  $\mu\text{L}$  of detergent dimethyl sulfoxide (Centralchem) was added to stop the reaction, and the absorbance was measured at 570 nm by a revelation microplate reader (Dynex MRX-TC). The percentage of metabolically active bacterial cells was calculated in relation to the positive control (100%).

## 2.6 | Bacterial membrane integrity

Plasma-induced damages to bacteria membrane integrity were determined by the propidium iodide (PI) uptake assay.<sup>[30]</sup> First, 1 mL of the sample was mixed with 10  $\mu\text{L}$  of 1.5 mM PI (Sigma-Aldrich) and incubated for 15 min at room temperature (RT) in the dark. The fluorescence intensity was measured at excitation and emission wavelengths of 535 and 636–652 nm, respectively. The percentage of the remaining cells with intact membranes was calculated in relation to the positive control (100%). Second, cells were stained separately with PI for cells with damaged membranes and 4',6-diamidino-2-phenylindole (DAPI; Sigma-Aldrich) for a total bacteria population to visualize by fluorescence microscopy (Intraco Micro LM 600). One milliliter of the sample was mixed with 200  $\mu\text{L}$  of 0.3 mM PI solution and incubated for 15 min at RT in the dark. The cell samples were washed thoroughly in saline to remove free probes before visualization. DAPI staining was performed by mixing 10  $\mu\text{L}$  of 300 nM DAPI solution with 5  $\mu\text{L}$  of sample followed by immediate visualization. Excitation filters GREEN (exciter filter BP510-550, dichroic mirror DM570, barrier filter 510) and UV (exciter filter BP330-

385, dichroic mirror DM400, barrier filter 420) were used allowing the detection of PI and DAPI fluorescent signals, respectively.

## 2.7 | Intracellular ROS

The accumulation of intracellular ROS was detected with the cell-permeant 2',7'-dichlorodihydrofluorescein diacetate ( $\text{H}_2\text{DCFDA}$ ) (Sigma-Aldrich) (adapted from Liao et al.<sup>[31]</sup>). The nonfluorescent  $\text{H}_2\text{DCFDA}$  may convert to the highly fluorescent 2',7'-dichlorofluorescein upon cleavage of the acetate groups by intracellular esterases and subsequent oxidation. One microliter of 1 mM  $\text{H}_2\text{DCFDA}$  was added to 1 mL of the bacterial suspensions; therefore, the final probe concentration in the aqueous solution was 10  $\mu\text{M}$ . After incubation for 30 min at 37°C in the dark and cell washing steps, the fluorescence was measured at excitation and emission wavelengths 488 and 526 nm, respectively. The intracellular ROS concentration was expressed as a relative ROS concentration, given by a formula =  $F/F_0 \times 100\%$ , where  $F_0$  and  $F$  are the fluorescence intensities of the bacterial suspension before and after plasma treatment, respectively.

## 2.8 | Bacterial morphology

Morphological cell damages were investigated by scanning electron microscope (SEM). First, cells collected from the sample suspension by centrifugation were transferred to 1.5 mL tubes and fixed in 4% paraformaldehyde (Sigma-Aldrich) for 1 h in the dark. These samples were then washed twice with PBS and sterile DI water for 10 min at room temperature (RT) before they were postfixed in 1% osmium tetroxide ( $\text{OsO}_4$ ) for 2 h in the dark. The samples were again washed twice in PBS and DI for 10 min, followed by dehydration steps consequently in 25%, 50%, 75%, and 95% ethanol for 10 min each and twice in 100% ethanol for 15 min.<sup>[32]</sup> Upon dehydration in 100% ethanol, 5  $\mu\text{L}$  of each sample was placed into the Si substrate and dried at RT. Before sputtering the polished Si (100) substrates were sonicated in acetone, isopropanol, and DI for 5 min and dried. The fixed samples were then viewed under a focused ion beam/scanning electron microscope (Tescan Lyra3) with an accelerator voltage of 5 – 10 kV.

## 2.9 | Statistical analysis

Each experiment was conducted independently a minimum of three times. Data were processed using Microsoft

Excel. One-way analysis of variance was performed to compare the results of microbiological cell enumeration from experimental groups with control groups and each against one other. A  $p$  value  $<0.05$  was considered statistically significant. All treatment values are presented as the mean  $\pm$  standard deviation (SD).

### 3 | RESULTS AND DISCUSSION

#### 3.1 | Physicochemical properties of PTL

##### 3.1.1 | Physical properties of PTL

Saline was treated by TS discharge, and the changes in temperature  $T$ , electrical conductivity  $\sigma$ , pH, and ORP were monitored immediately after the treatment. Figure 2 illustrates the given physical properties of PTL during 20 min of plasma treatment. The temperature slowly increased from the initial 20°C up to 32°C (Figure 2a). The initial  $\sigma$  was 6.4 mS/cm and did not change significantly during plasma treatment (Figure 2a). In a previous and similar study, we observed negligible  $T$  increase and  $\sigma$  increase by 0.7 mS/cm after 10 min TS discharge treatment of saline.<sup>[33]</sup> We also tested TS discharge with electrospray of saline and found  $\sigma$  increased by 0.5 mS/cm after 5 min plasma treatment.<sup>[24]</sup>

Strong acidification of PTLs is typical for nonbuffered solutions (i.e., saline or DI). We observed that pH gradually decreased over 20 min from initial 5.8 to 2.4 (Figure 2b). In general, pH value is being reported as critical for bacterial inactivation. Chandana et al.<sup>[34]</sup> observed a significant log reduction achieved for 150 s on *E. coli* treated by Ar/air plasma jet and for pH was below 4.7. The same critical pH was also reported by Ikawa et al.<sup>[35]</sup> who obtained total inactivation of bacteria after 120 s for *E. coli* and even acidophilic *Leuconostoc citreum* treated by He LF plasma jet. Chen et al.<sup>[36]</sup> identified the

critical pH 2 of PTL for the antibacterial and antibiofilm activity of *E. coli*, which were not inactivated above the critical pH. Copper and zinc ions in PTL from the cathode under acidic conditions played a key role in inactivation.

The change in pH is often associated with a change in ORP. While pH indicates how acidic or basic a solution is the ORP indicates changes of oxidizing or reducing agents. In our case, the initial ORP of 304 mV increased by the 15th min to 347 mV (Figure 2b). The observed unstable trend for ORP may be attributed to the postplasma occurring reactions. Nevertheless, measured ORP is low to cause strong oxidation in comparison to other studies. For instance, treated by plasma jet saline with ORP of  $\sim 800$  mV in 20 min was reported,<sup>[19]</sup> also for 20 min plasma jet treatment of DW resulted in ORP of 550 mV,<sup>[37]</sup> and just 1 min plasma jet treatment of DW was enough to reach ORP of 576 mV.<sup>[38]</sup> The measurements of pH and ORP in PTL are associated with the formation of RONS. Therefore, acidification and high ORP levels are an indicator of potential bactericidal efficacy.<sup>[39,40]</sup>

##### 3.1.2 | Chemical composition of PTL

The concentrations of long-lived species, namely,  $\text{NO}_2^-$ ,  $\text{NO}_3^-$ , and  $\text{H}_2\text{O}_2$ , and short-lived  $\bullet\text{OH}$  and  $\text{ONOO}^-$  in PTL during 20 min of plasma treatment are shown in Figure 3. When the TS discharge is generated in ambient air, it mainly produces NO and  $\text{NO}_2$ , as well as  $\text{HNO}_2$ . Their further dissolution in PTL, in particular  $\text{HNO}_2$ , leads to its acidification.<sup>[41]</sup> After 20 min, the concentrations of  $\text{H}_2\text{O}_2$  and  $\text{NO}_3^-$  in PTL reached 2.54 and 2.18 mM, respectively (Figure 3a). A small amount of  $\text{NO}_2^-$  was produced at the beginning of treatment (0.29 mM for 5 min), followed by its gradual decomposition into  $\text{NO}_3^-$  under acidic conditions (pH  $< 3.2$ ).  $\text{NO}_2^-$  could also react

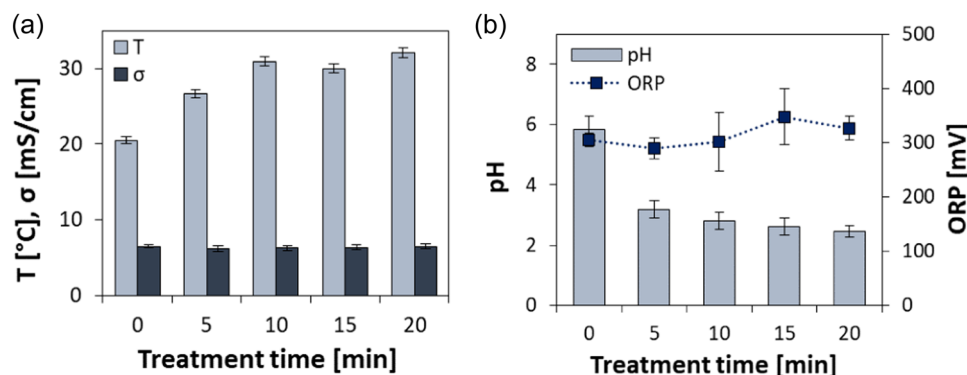


FIGURE 2 Physical properties of plasma-treated liquid in terms of (a) temperature, and conductivity; (b) pH, oxidation–reduction potential as a function of plasma treatment time.

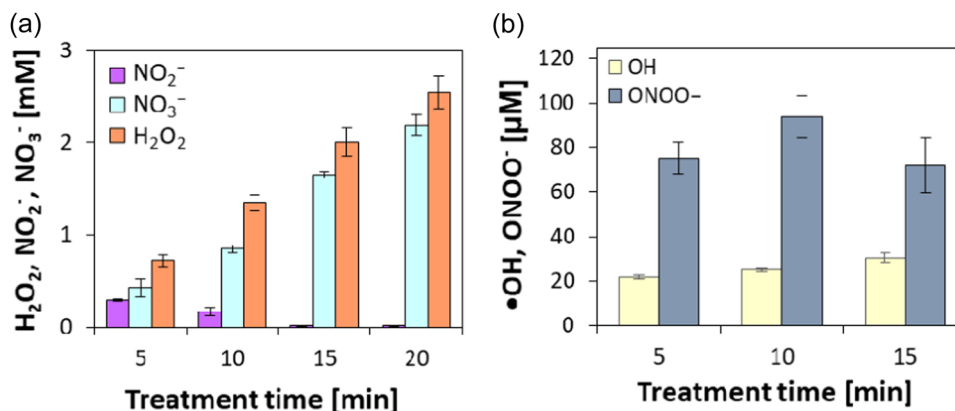


FIGURE 3 Concentrations of (a)  $\text{NO}_2^-$ ,  $\text{NO}_3^-$ , and  $\text{H}_2\text{O}_2$  and (b) the total amounts of  $\bullet\text{OH}$ ,  $\text{ONOO}^-$  accumulated in plasma-treated liquid as a function of plasma treatment time.

with  $\text{H}_2\text{O}_2$  leading to the formation of intermediate peroxyntrous acid  $\text{O}=\text{NOOH}$ . Detected  $\text{ONOO}^-$  concentrations (Figure 3b) first increased ( $\sim 94 \mu\text{M}$  for 10 min), and then were dominated by  $\text{O}=\text{NOOH}$  in the acidic conditions.  $\text{O}=\text{NOOH}$  could further decompose into  $\text{NO}_3^-$  and  $\bullet\text{OH}$ . The concentration of  $\bullet\text{OH}$  increased with increasing treatment time ( $\sim 30 \mu\text{M}$  for 15 min).

Our previously published results on PTL generated by TS discharge in two configurations demonstrated comparable trends for RONS concentrations. In nonbuffered water solutions (DI, saline) treated by TS discharge with water electro spray, an accumulation of  $\text{NO}_2^-$  (0.2 mM),  $\text{NO}_3^-$  ( $\sim 0.9$  mM), and  $\text{H}_2\text{O}_2$  (0.7 mM) was observed.<sup>[24]</sup> For DI treated by the presented system with water electrode (Figure 1a) concentrations of  $\text{NO}_2^-$  (0.27 mM),  $\text{NO}_3^-$  (0.57 mM), and  $\text{H}_2\text{O}_2$  ( $\sim 0.85$  mM) were reported.<sup>[42]</sup> In a similar study, Hansch et al.<sup>[43]</sup> used DBD above a saline surface and reported changes in chemical composition of PTL, namely, the prevalence of  $\text{NO}_3^-$  ( $\sim 2.7$  mM), with smaller amounts of  $\text{NO}_2^-$  (0.09 mM) and  $\text{H}_2\text{O}_2$  (0.03 mM) after 6 min treatment. The generation of RONS depends on the type of plasma discharge and treated liquid. For example, different trends of reactive species generation in PTL were reported by Machala et al.<sup>[44]</sup> for streamer corona and TS discharges. Domination of  $\text{NO}_2^-$  ( $\sim 0.3$  mM),  $\text{NO}_3^-$  ( $\sim 1.35$  mM), and  $\text{H}_2\text{O}_2$  ( $\sim 0.7$  mM) in TS discharge generated PTL were detected compared to streamer corona discharge for which high concentrations of  $\text{O}_3$  and  $\text{H}_2\text{O}_2$  ( $\sim 0.45$  mM) were detected.

In addition, plasma-induced oxychlorine chemistry might take place when saline is treated. However, saline solutions are preferably used for microbiological analysis to provide an iso-osmotic medium for the prevention of bacteria destruction caused by osmotic effects. In PTLs, the formation of hypochlorite ( $\text{ClO}^-$ ) must be taken into

consideration, which is well known for its antimicrobial activity. In our experiments, the concentration of  $\text{Cl}^-$  remained unchanged at the level of  $\sim 6$  mM. Analysis of PTL for  $\text{OCl}^-$  did not show any significant spectral difference, seemingly indicating reactive chlorine species were not generated. Similarly, Oehmigen et al.<sup>[45]</sup> also reported no change in  $\text{Cl}^-$  concentration for DBD-treated saline for 7 min. Researchers observed continually increased  $\text{H}_2\text{O}_2$  and  $\text{NO}_3^-$ , and temporarily increasing  $\text{NO}_2^-$  as in our experiments. It was suggested that reactions of gas-phase molecules like  $\text{N}_2\text{O}$ , ozone  $\text{O}_3$ ,  $\text{CO}_2$ ,  $\text{HNO}_3$ , and/or  $\text{ONOOH}$  with the aqueous liquid might cause the appearance of less stable but biologically active chemical intermediates like  $\text{NO}\bullet$  or  $\text{NO}_2\bullet$ ,  $\bullet\text{OH}$ , or  $\text{HOO}\bullet$ . On the contrary,  $\text{OCl}^-$  was found a major liquid-phase product in plasma-treated saline in closed, dry conditions without access to ambient air.<sup>[19]</sup>

### 3.2 | Bacterial viability

TS discharge plasma showed high bactericidal efficacy on *E. coli* and *S. aureus* suspended in saline both in *stat* and *exp* growth phases. The decrease of a bacterial population expressed in the log reduction is depicted in Figure 4. Different inactivation kinetics were observed for *E. coli* and *S. aureus*. For Gram<sup>-</sup> *E. coli* 15 min treatment resulted in a total bacterial inactivation (Figure 4a). Gram<sup>+</sup> *S. aureus* appeared more resistant to plasma treatment as  $\sim 3$  log reduction was achieved for up to 20 min treatment in a time-independent manner (Figure 4b). The results can be explained based on different cell envelope structures and are in agreement with the majority of other studies. Intriguing defense mechanisms of Gram-opposite bacteria against ROS in PTL were proposed by Schnabel et al.<sup>[46]</sup> Because of more

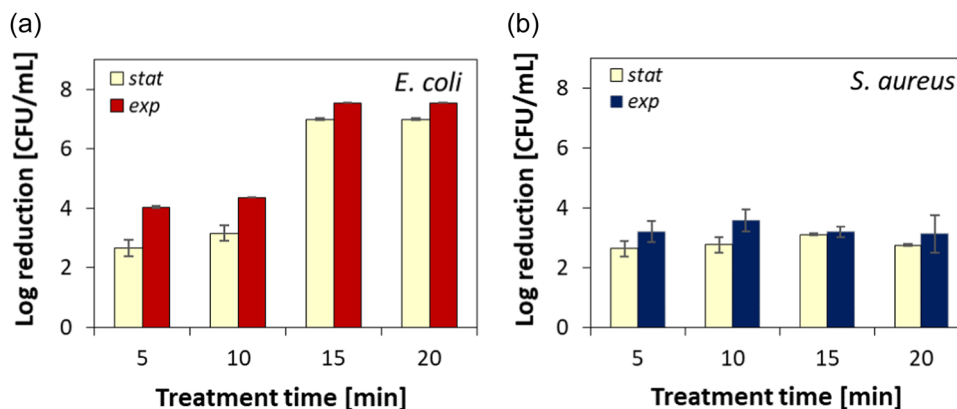


**FIGURE 4** Bactericidal effect on planktonic (a) *Escherichia coli* and (b) *Staphylococcus aureus* in saline during stationary (*stat*) and exponential (*exp*) growth phase as a function of plasma treatment time.

periplasmic space with superoxide dismutase (SOD) Gram<sup>-</sup> bacteria are suggested to be more resistant against O<sub>2</sub><sup>•-</sup> and less resistant against H<sub>2</sub>O<sub>2</sub> due to less peptidoglycan compared to Gram<sup>+</sup> bacteria. It is explained by the reaction of SOD that takes place in the periplasm converting O<sub>2</sub><sup>•-</sup>, and the inability of H<sub>2</sub>O<sub>2</sub> to easily diffuse through a layer of peptidoglycan. Also, reactive nitrogen species (RNS) from PTL were proposed to influence bacteria differently. For example, due to a larger periplasm of Gram<sup>-</sup> bacteria reductases degrade NO<sub>3</sub><sup>-</sup> providing more efficient protection against RNS. Whereas Gram<sup>+</sup> bacteria have less periplasmic space where the NO<sub>3</sub><sup>-</sup> concentration is higher and bacterial defense reactions are slower. For instance, Gram<sup>-</sup> *E. coli* (6.5 log) demonstrated less resistance to the atmospheric pressure DC air plasma compared to Gram<sup>+</sup> *S. aureus* (5.3 log).<sup>[47]</sup> Similarly, Gram<sup>-</sup> *S. Typhimurium* was less resistant to DBD plasma treatment than Gram<sup>+</sup> *S. aureus*.<sup>[8]</sup> With a 100-s treatment, the bactericidal effect resulted in a 3.2 log and 1.8 log reduction for *S. Typhimurium* and *S. aureus*, respectively. Likewise, PTL generated by plasma jet caused a stronger bactericidal effect on a number of Gram<sup>-</sup> bacteria compared to Gram<sup>+</sup> species.<sup>[48]</sup>

For both strains, a slightly stronger bactericidal effect was observed in the *exp* growth phase where plasma treatment led to 4.3 and 3.5 log reduction for a 10 min treatment time of *E. coli* and *S. aureus*, respectively (Figure 4). For the same treatment time in the *stat* phase, counts of *E. coli* decreased by 3.1 log, and *S. aureus* by 2.7 log. The lower resistance of bacteria in the *exp* phase was probably due to the growing physiology of “young” cells when high metabolic activity is maintained. On the contrary, nongrowing “mature” cells in the *stat* phase were more resistant to high-stress environment factors. The dependence of bacterial resistance to plasma on the growth phase was also investigated

by Yu et al.<sup>[49]</sup> In their study, *E. coli* exhibited a higher level of resistance in the *stat* phase (~2.5 log) compared to mid- and late-*exp* phase (3–4 log) cells. Similarly, *E. coli* resistance to plasma increased at the transition from *exp* to *stat* phase, where the population survival was ~95% and ~30%, respectively.<sup>[50]</sup> Authors connected the effect to cell adaptation to the environment (nutrient depletion, accumulation of waste material, and congestion). The literature identifies higher resistance of *stat* phase bacteria for other treatments as well. For example, DNA-binding protein in *stat*-phase *E. coli* has been suggested to be responsible for cell protection from multiple stresses, such as UV and  $\gamma$ -irradiation, iron and copper toxicity, thermal and oxidative stress, and acid and base shock.<sup>[51]</sup> To study the plasma-induced mechanisms of bacterial inactivation in detail, *exp*-phase cells were chosen for further analysis as we found them to be more sensitive to TS discharge in our experiment.

Moreover, the posttreatment bactericidal effect was estimated by incubating bacteria in PTL for a given time after switching off the discharge. Results shown in Figure 5 were obtained for bacterial suspensions treated directly by TS discharge for 5 min and subsequently incubated for 15–120 min. Plasma-generated RONS in PTL facilitated the increase of bacterial inactivation with increasing incubation time. After 120 min *E. coli* was completely inactivated, and *S. aureus* reached ~5 log reduction.

### 3.3 | Bacterial metabolic activity

To elucidate bacterial metabolism and examine the presence of potentially viable cells, metabolic activity was measured. Figure 6 shows detected changes in enzyme activities, proving the reduced metabolic activity. After 5 min treatment, 42% of *E. coli* cells remained

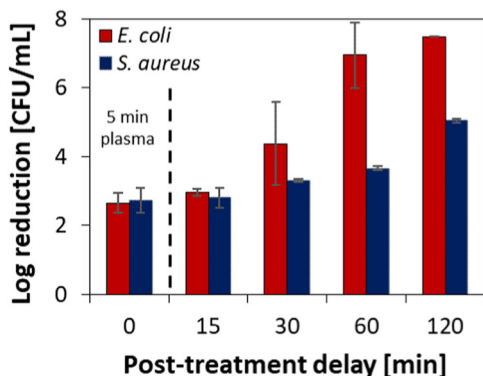


**FIGURE 5** Postplasma-delayed bactericidal effect on *Escherichia coli* and *Staphylococcus aureus* after 5 min plasma treatment time, followed by incubation in PTL (bacteria in *stat* growth phase).

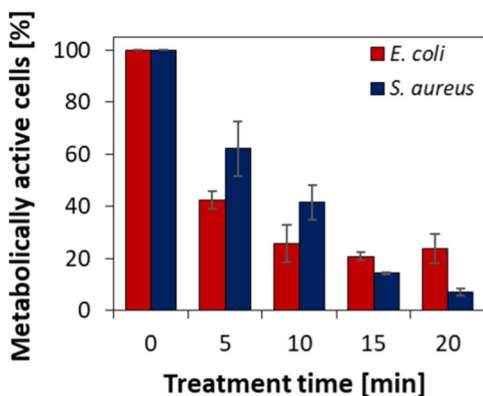


**FIGURE 6** Metabolic activity of and *Escherichia coli* and *Staphylococcus aureus* in saline as a function of plasma treatment time (bacteria in the *exp* growth phase).

metabolically active, whereas 20 min reduced this number to 23%. Metabolically active *S. aureus* cells after 5 min decreased to only 62%, but after 20 min plasma treatment, it was as low as 7%. The percentage of *S. aureus* metabolically active cells displayed a sigmoid-like decreasing tendency, while the quick decrease of metabolically active *E. coli* in the first 5 min of treatment remained fairly stable.

Percentage reduction based on MTT assay showed a good correlation with viability assay for *S. aureus* with 3.2 log (Figure 4b), and 14% of metabolically active cells (Figure 6) were detected after 15 min treatment. In the case of *E. coli*, 21% of metabolically active cells were detected with the same treatment time, while the viability assay showed undetectable colony count levels (Figure 4a). A residual metabolic activity of *E. coli* might be due to a viable but nonculturable (VBNC) state as a result of oxidative stress from plasma-generated RONS. Bacteria go into a survival state with probable

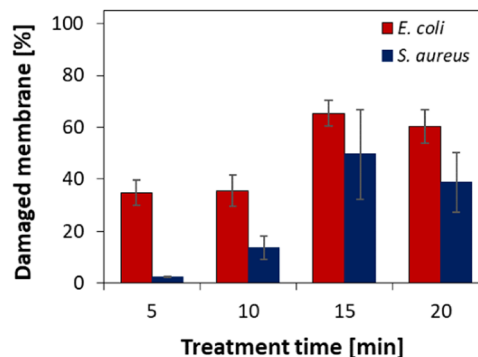


**FIGURE 7** Membrane integrity of *Escherichia coli* and *Staphylococcus aureus* in saline as a function of plasma treatment time (bacteria in the *exp* growth phase).

morphological changes, cell wall composition, respiratory activity, gene transcription, and protein synthesis, but are not capable of growing on media.<sup>[52]</sup> It is known that plasma-exposed cells can survive despite the suppression of their metabolic functions.<sup>[53]</sup> This was also observed by Cooper et al.<sup>[54]</sup>, who found that *Bacillus stratosphericus* entered the VBNC state after being exposed to DBD plasma. A relatively high XTT (2,3-bis-(2-methoxy-4-nitro-5-sulphophenyl)-2H-tetrazolium-5-carboxanilide) activity was detected even 24 h after plasma treatment, although the cells could not form colonies on the culture media. In another study,<sup>[55]</sup> 34% of *E. coli* from the biofilm were found metabolically active after DBD exposure, while the plate count showed total bacterial inactivation (8 log). Interestingly, for *Listeria monocytogenes*, *S. aureus*, and *Pseudomonas fluorescens*, the XTT assay correlated with the viability results. Treatment for 60 s resulted in nearly 4 log reduction, with ~30%–60% of metabolically active cells remaining.

### 3.4 | Bacterial membrane integrity

The membrane integrity of plasma-treated *S. aureus* and *S. aureus* was examined using PI and DAPI fluorescence dyes. Figure 7 represents the trends of losing the membrane integrity in the percentage of nonstained intact cells. The greater ability to preserve the integral membrane was found for *S. aureus*. The gradual decrease of membrane integrity with a maximum damage of 49% for 15 min plasma treatment was detected. *E. coli* rapidly lost 35% of integral cells in 5 min and reached its maximum of 65% in 15 min treatment. Interestingly, in the *stat* growth phase, merely 22% of damaged *E. coli* were detected, while negligible damage (>1%) was observed for *S. aureus*

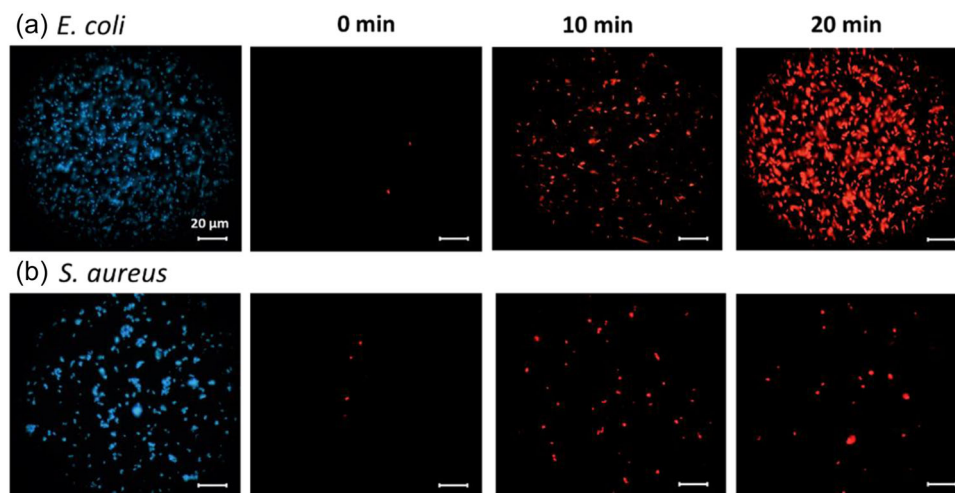


**FIGURE 8** Visualization of 4',6-diamidino-2-phenylindole (DAPI) and propidium iodide (PI) staining of planktonic *Escherichia coli* and *Staphylococcus aureus* in saline (bacteria in the *exp* growth phase) by fluorescence microscopy as a function of plasma treatment; bar is 20  $\mu\text{m}$ . The blue cells indicate a total bacteria population. The red cells indicate bacteria with damaged membranes (PI penetration).

after a maximum 20 min treatment (data are not shown). This result proves that the increased stress resistance of bacteria after entering the *stat* growth phase is due to the development of stronger cell envelopes. A recent study by Huang et al.<sup>[8]</sup> confirmed the higher membrane damages toward Gram<sup>-</sup> *S. Typhimurium* than Gram<sup>+</sup> *S. aureus*. DBD treatment for 100 s induced ~92% and ~54% damages for *S. Typhimurium* and *S. aureus*, respectively.

Fluorescence images of the PI- and DAPI-stained planktonic *E. coli* and *S. aureus* are depicted in Figure 8. DAPI staining was performed to demonstrate the total number of bacteria in control. The number of red membrane-damaged *E. coli* cells in relation to a total population substantially increased with prolonged plasma treatment time. On the contrary, treatment time did not affect the count of red-stained *S. aureus*. Around ~30% of PI-stained cells remained for *S. aureus* from 5 to 20 min treatment. The values of PI/DAPI (%) ratios calculated from the total fluorescence area revealed similar spectroscopic measurement trends of the uptake of PI alone (Figure 9).

The notable difference between *E. coli* and *S. aureus* indicates the importance of cell membranes for effective inactivation by plasma. Our results prove that components of the outer membrane (phospholipids, LPSs, and lipoproteins) of Gram<sup>-</sup> bacteria have a greater susceptibility to RONS, while the same species hardly break bonds in a thick peptidoglycan layer of Gram<sup>+</sup> ones.<sup>[56]</sup> Thus, the outer membrane in Gram<sup>-</sup> *E. coli* played an essential role in targeting the membrane integrity by RONS produced by TS discharge.

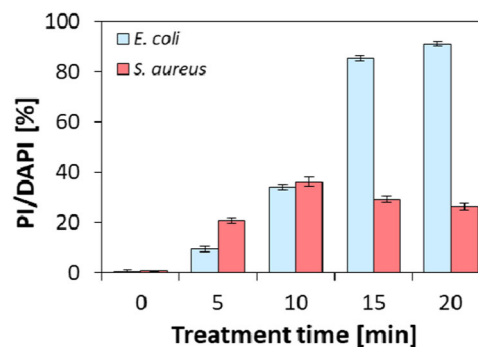


**FIGURE 9** Quantification of dead bacteria as a relative change of average total fluorescence area propidium iodide/4',6-diamidino-2-phenylindole (%) based on signals obtained by fluorescence microscopy.

### 3.5 | Intracellular ROS

Intracellular ROS concentrations were measured to evaluate oxidative stress (intracellular redox state) in bacteria caused by plasma-generated reactive species. Figure 10 shows the intracellular ROS concentrations for the plasma-treated bacteria. For *E. coli* intracellular ROS level was radically increased by 428% after 5 min plasma treatment. After reaching the maximum concentration, the intracellular ROS level decreased to 170% and remained fairly stable up to the 20th min. Unlike *E. coli*, *S. aureus* did not accumulate intracellular ROS. Unusually, the disturbed cells' redox balance lowered intracellular ROS levels. After 5 min of treatment, intracellular ROS level decreased to 48% and further did not change by more than 10%.

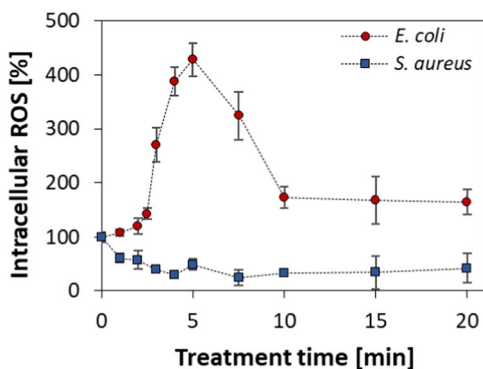


**FIGURE 10** Relative overall intracellular ROS concentrations of *Escherichia coli* and *Staphylococcus aureus* as a function of plasma treatment (bacteria in the *exp* growth phase; plasma-untreated sample set to 100%).

Similar results have been previously observed, demonstrating that plasma can induce oxidative stress in bacteria.<sup>[57]</sup> However, our findings conflict with several other studies that reported significant accumulation of intracellular ROS after plasma treatment, especially in Gram<sup>+</sup> bacteria, where a higher increase is usually observed in comparison with Gram<sup>-</sup> ones. Several authors have considered the connection between damaged membranes and intracellular ROS leakage after its accumulation. Xu et al.<sup>[47]</sup> reported plasma-induced accumulation of maximum intracellular ROS by 132% (5 min) and 218% (10 min) for *E. coli* and *S. aureus*, respectively, treated by DC corona discharge and followed by its decrease. The same trend was observed for *S. aureus* treated by DBD plasma combined with ultrasound,<sup>[31]</sup> where maximum ROS level was achieved within 10 min followed by its decrease. Likewise, a plasma jet treatment under the water surface resulted in the accumulation of intracellular ROS of *S. aureus* by 300% (15 min) with its subsequent decrease.<sup>[58]</sup> An interesting insight was presented by Han et al.<sup>[9]</sup> who compared the ROS accumulation in *E. coli* and *S. aureus* for direct and indirect DBD treatments. Similar to the studies above, for direct treatment the increase of intracellular ROS by 400% (3 min) was observed followed by its decrease. However, for indirect treatment, both bacteria showed a gradual accumulation of intracellular ROS without its leakage.

An increase in intracellular ROS production is usually observed in bacteria exposed to various oxidative treatments. For example, a similar effect was detected for *E. coli* exposed to photodynamic therapy (PDT).<sup>[59]</sup> CuO NPs and silver-functionalized copper oxide (Ag@CuO) nanocomposites induced intracellular ROS generation in *E. coli*, *Salmonella enterica*, and *S. aureus*.<sup>[60]</sup> PDT conjugated with ZnO NPs induced an increase in *S. aureus* intracellular ROS by about 200%.<sup>[61]</sup>

### 3.6 | Bacterial morphology

SEM was applied for the investigation of the morphological changes of bacteria after being exposed to TS discharge for 15 min. The SEM images show plasma-induced damage to *E. coli* and *S. aureus* cells. Untreated *E. coli* cells were regular, plump with smooth surfaces, and rod-shaped morphology (Figure 11a). Multiple surface damages detected in *E. coli* treated by TS discharge are shown in Figure 11b–f. Detected previously by fluorescence techniques, disruption of membranes is visually confirmed here (Figure 11b). Consequent leakage of intracellular components was observed (Figure 11c). Other cell deformations include cell segregation, cell wreckage, and cell clumping. Similarly, untreated *S. aureus* displayed typical spherical morphology with full surfaces, uniform in size (Figure 11g). However, *S. aureus* treated with TS discharge exhibited slight deformations, accompanied by the appearance of a larger amount of extracellular vesicles (EVs) compared to intact cells (Figure 11h–l). Also, sporadic cases of the EVs release were observed for *E. coli* (Figure 11e). Presumably, this plays a protective role in response to plasma treatment. Furthermore, the observed uniform distribution of released EVs on *S. aureus* might be one of the reasons for higher resistance to plasma. Our result is in agreement with numerous studies that emphasize severe morphological changes for Gram<sup>-</sup> bacteria and fewer or unnoticeable changes for Gram<sup>+</sup> bacteria after the plasma treatment.<sup>[62–64]</sup> For instance, Laroussi et al.<sup>[65]</sup> stressed the role of electrostatic disruption of the outer cell membrane of Gram<sup>-</sup> *E. coli*. In their study, SEM revealed cell lysis of *E. coli* and no morphological changes in Gram<sup>+</sup> *B. subtilis*.

To sum up, the obtained results demonstrate that plasma treatment diversely altered the external structures of tested bacteria and caused irreversible damage to *E. coli* cell walls and membranes, which accelerated cell death. The shape of bacterial cells can therefore influence the inactivation effect of plasma, with spherical cells (cocci) being more resistant to plasma than rod-shaped cells (bacilli).

## 4 | CONCLUSION

We studied the effects of TS discharge on Gram<sup>-</sup> *E. coli* and Gram<sup>+</sup> *S. aureus* bacteria in saline solution and compared the inactivation mechanisms. TS discharge showed a high bactericidal efficacy and induced up to 7 log and 3 log reductions within 15 min plasma treatment of *E. coli* and *S. aureus*, respectively. A slightly higher inactivation was observed for bacteria in the *exp* growth phase than in the *stat* growth phase, highlighting

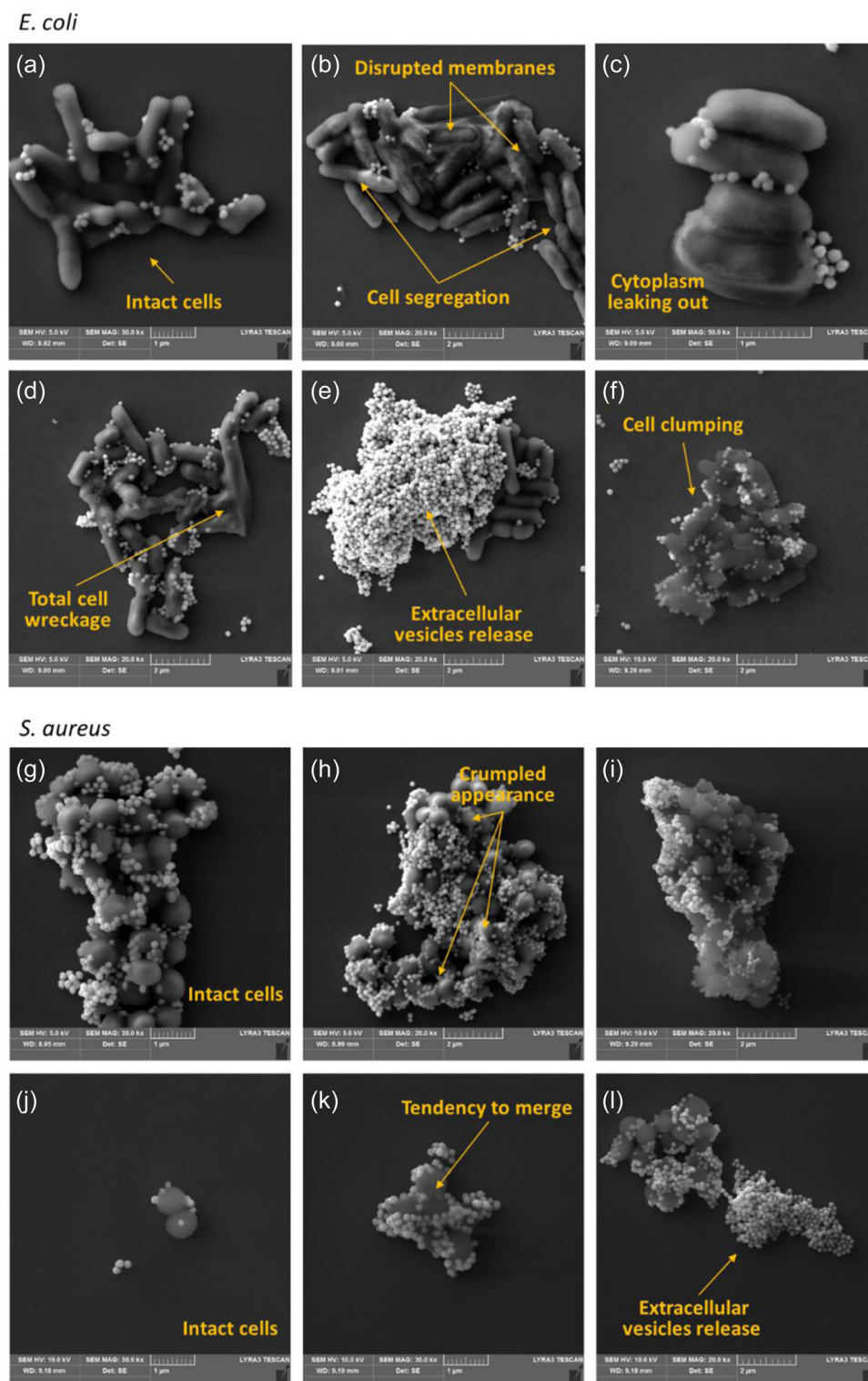


**FIGURE 11** Effects of plasma treatment on cell morphology analyzed by scanning electron microscope: (a)–(f) *Escherichia coli* and (g)–(l) *Staphylococcus aureus*. Plasma treatment time 15 min. Arrows indicate damages on the cell surface.

lower resistance of cells toward plasma during their growing phase (*exp* phase) with a high level of metabolic activity. Interestingly, a strong reduction of metabolic activity of *S. aureus* by 93% did not cause a total inactivation, whereas total inactivation of *E. coli*

corresponded to only a 77% reduction. The discrepancy of bactericidal effect with metabolic activity in the case of *E. coli* might be due to VBNC state phenomena. Different mechanisms of inactivation were observed for Gram<sup>-</sup> *E. coli* and Gram<sup>+</sup> *S. aureus*. Plasma-generated

reactive species were found to destroy the cell membrane of *E. coli* facilitating the rapid accumulation of intracellular ROS followed by a collapse of intracellular redox balance. Moreover, multiple morphological damages were confirmed for plasma-treated *E. coli*. On the contrary, *S. aureus* survived plasma treatment for even 20 min. We suggest the preservation of the cell membrane and morphological integrity provided protection from plasma-generated reactive species, leading to the survival pathway of *S. aureus*. •OH, H<sub>2</sub>O<sub>2</sub>, ONOOH, and NO<sub>3</sub><sup>-</sup> combined with acidic pH and increased ORP facilitated the bactericidal effect of the TS discharge. Posttreatment incubation in PTL caused an increase in bacterial inactivation, indicating a contribution of plasma-generated long-lived RONS in bactericidal effect. Altogether, the bactericidal efficacy of TS discharge depends on the type of bacteria, its growth phase, and the physicochemical properties of its surrounding environment.

### AUTHOR CONTRIBUTIONS

**Conceptualization:** Aleksandra Lavrikova and Karol Hensel. **Validation:** Aleksandra Lavrikova, Karol Hensel, and Helena Bujdaková. **Project management:** Karol Hensel. **Investigation:** Aleksandra Lavrikova. **Experiments' performance:** Aleksandra Lavrikova and Nitin Chandra Teja Dadi. **Writing—original draft preparation:** Aleksandra Lavrikova. **Writing—review and editing:** Karol Hensel

### ACKNOWLEDGMENTS

The authors would like to thank Leonid Satrapinsky and Hryhorii Makarov for their help with the SEM analysis. This research was funded by Slovak Research and Development Agency (APVV-20-0566 and APVV-22-0247), Slovak Grant Agency (VEGA 1/0596/22), and by “PlasTHER” COST Action (CA20114) (supported by European Cooperation in Science and Technology).

### CONFLICT OF INTEREST STATEMENT

The authors declare no conflict of interest.

### DATA AVAILABILITY STATEMENT

The data that support the findings of this study are available on request from the corresponding author. The data are not publicly available due to privacy or ethical restrictions.

### ORCID

Aleksandra Lavrikova  <https://orcid.org/0000-0002-8510-6503>

Helena Bujdaková  <https://orcid.org/0000-0002-9219-0803>

Karol Hensel  <http://orcid.org/0000-0001-6833-681X>

### REFERENCES

- [1] E. Sanganyado, W. Gwenzi, *Sci. Total Environ.* **2019**, 669, 785.
- [2] I. Niedźwiedz, A. Waško, J. Pawlat, M. Polak-Berecka, *Pol. J. Microbiol.* **2019**, 68, 153.
- [3] A. Khlyustova, C. Labay, Z. Machala, M.-P. Ginebra, C. Canal, *Front. Chem. Sci. Eng.* **2019**, 13, 238.
- [4] N. K. Kaushik, B. Ghimire, Y. Li, M. Adhikari, M. Veerana, N. Kaushik, N. Jha, B. Adhikari, S.-J. Lee, K. Masur, T. von Woedtke, K.-D. Weltmann, E. H. Choi, *Biol. Chem.* **2018**, 400, 39.
- [5] P. Bourke, D. Ziuzina, L. Han, P. J. Cullen, B. F. Gilmore, *J. Appl. Microbiol.* **2017**, 123, 308.
- [6] M. Yusupov, A. Bogaerts, S. Huygh, R. Snoeckx, A. C. T. van Duin, E. C. Neyts, *J. Phys. Chem. C* **2013**, 117, 5993.
- [7] E. A. J. Bartis, P. Luan, A. J. Knoll, D. B. Graves, J. Seog, G. S. Oehrlein, *Plasma Process. Polym.* **2016**, 13, 410.
- [8] M. Huang, H. Zhuang, J. Zhao, J. Wang, W. Yan, J. Zhang, *Bioelectrochemistry* **2020**, 132, 107445.
- [9] L. Han, S. Patil, D. Boehm, V. Milosavljević, P. J. Cullen, P. Bourke, *Appl. Environ. Microbiol.* **2016**, 82, 450.
- [10] J. A. Imlay, *Annu. Rev. Microbiol.* **2003**, 57, 395.
- [11] C. Nathan, A. Ding, C. Nathan, A. Ding, *Cell* **2010**, 140, 871.
- [12] M. J. Zhao, L. Jung, C. Tanielian, R. Mechin, *Free Radic. Res.* **1994**, 20, 345.
- [13] E. Sysolyatina, A. Mukhachev, M. Yurova, M. Grushin, V. Karalnik, A. Petryakov, N. Trushkin, S. Ermolaeva, Y. Akishev, *Plasma Process. Polym.* **2014**, 11, 315.
- [14] S. G. Joshi, M. Cooper, A. Yost, M. Paff, U. K. Ercan, G. Fridman, G. Friedman, A. Fridman, A. D. Brooks, *Antimicrob. Agents Chemother.* **2011**, 55, 1053.
- [15] B. G. Rodriguez-Mendez, A. N. Hernandez-Arias, R. Lopez-Callejas, R. Valencia-Alvarado, A. Mercado-Cabrera, R. Pena-Eguiluz, S. R. Barocio-Delgado, A. E. Munoz-Castro, A. de la Piedad-Beneitez, *IEEE Trans. Plasma Sci.* **2013**, 41, 147.
- [16] R. Zhou, R. Zhou, K. Prasad, Z. Fang, R. Speight, K. Bazaka, K. Ostrikov, *Green Chem.* **2018**, 20, 5276.
- [17] Z. Ke, P. Thopan, G. Fridman, V. Miller, L. Yu, A. Fridman, Q. Huang, *Clin. Plasma Med.* **2017**, 7–8, 1.
- [18] K. Kučerová, Z. Machala, K. Hensel, *Plasma Chem. Plasma Process.* **2020**, 40, 749.
- [19] V. Jirásek, P. Lukeš, *Plasma Sources Sci. Technol.* **2019**, 28, 035015.
- [20] Y. Gorbanev, J. Van der Paal, W. Van Boxem, S. Dewilde, A. Bogaerts, *Phys. Chem. Chem. Phys.* **2019**, 21, 4117.
- [21] K. Hensel, K. Kučerová, B. Tarabová, M. Janda, Z. Machala, K. Sano, C. T. Mihai, M. Ciorpac, L. D. Gorgan, R. Jijie, V. Pohoata, I. Topala, *Biointerphases* **2015**, 10, 029515.
- [22] M. Zdenko Machala, M. Marcela Morvová, M. Emmanuel Marode, M. Imrich Morva, *J. Phys. D.* **2000**, 33(no. 24), 3198.
- [23] M. Janda, V. Martišovitéš, Z. Machala, *Plasma Sources Sci. Technol.* **2011**, 20, 035015.
- [24] Z. Machala, B. Tarabova, K. Hensel, E. Spetlikova, L. Sikurova, P. Lukes, *Plasma Process. Polym.* **2013**, 10, 649.
- [25] B. Tarabová, L. Šikurová, P. Lukeš, M. Janda, Z. Machala, *Plasma Process. Polym.* **2018**, 15, e1800030.
- [26] F. Tampieri, M.-P. Ginebra, C. Canal, *Anal. Chem.* **2021**, 93, 3666.

- [27] T. J. Mason, J. P. Lorimer, D. M. Bates, Y. Zhao, *Ultrason. Sonochem.* **1994**, *1*, S91.
- [28] S. Kanazawa, T. Furuki, T. Nakaji, S. Akamine, R. Ichiki, *Int. J. Plasma Environ. Sci. Technol.*, **2012**, *6*, 166.
- [29] J. C. Stockert, R. W. Horobin, L. L. Colombo, A. Blázquez-Castro, *Acta Histochem.* **2018**, *120*, 159.
- [30] Y. Niu, S. Li, Z. Lin, M. Liu, D. Wang, H. Wang, S. Chen, *J. Chromatogr. A* **2016**, *1463*, 102.
- [31] X. Liao, J. Li, A. I. Muhammad, Y. Suo, J. Ahn, D. Liu, S. Chen, Y. Hu, X. Ye, T. Ding, *Food Control* **2018**, *90*, 241.
- [32] N. C. Dadi, M. Dohál, V. Medvecká, J. Bujdák, K. Kočí, A. Zahoranová, H. Bujdánková, *Molecules* **2021**, *26*, 325.
- [33] M. Schmidt, V. Hahn, B. Altmann, T. Gerling, I. C. Gerber, K.-D. Weltmann, T. von Woedtke, *Appl. Sci.* **2019**, *9*, 2150.
- [34] L. Chandana, C. J. Sangeetha, T. Shashidhar, C. h Subrahmanyam, *Sci. Total Environ* **2018**, *640–641*, 493.
- [35] S. Ikawa, K. Kitano, S. Hamaguchi, *Plasma Process. Polym.* **2010**, *7*, 33.
- [36] T. P. Chen, J. Liang, T. L. Su, *Environ. Sci. Pollut. Res.* **2018**, *25*, 26699.
- [37] R. Ma, G. Wang, Y. Tian, K. Wang, J. Zhang, J. Fang, *J. Hazard. Mater.* **2015**, *300*, 643.
- [38] Q. Xiang, C. Kang, D. Zhao, L. Niu, X. Liu, Y. Bai, *Food Control* **2019**, *99*, 28.
- [39] J. Shen, Y. Tian, Y. Li, R. Ma, Q. Zhang, J. Zhang, J. Fang, *Sci. Rep.* **2016**, *6*, 28505.
- [40] X. Lu, G. V. Naidis, M. Laroussi, S. Reuter, D. B. Graves, K. Ostrikov, *Phys. Rep.* **2016**, *630*, 1.
- [41] M. Janda, K. Hensel, P. Tóth, M. E. Hassan, Z. Machala, *Appl. Sci.* **2021**, *11*, 7053.
- [42] K. Kučerová, M. Henselová, L. Slovák, K. arol Hensel, *Plasma Process. Polym.* **2018**, *16*, e1800131.
- [43] M. A. C. Hänsch, M. Mann, K.-D. Weltmann, T. von Woedtke, *J. Phys. D* **2015**, *48*, 454001.
- [44] Z. Machala, B. Tarabová, D. Sersenová, M. Janda, K. Hensel, *J. Phys. D* **2019**, *52*, 034002.
- [45] K. Oehmigen, J. Winter, M. Hähnel, C. Wilke, R. Brandenburg, K.-D. Weltmann, T. von Woedtke, *Plasma Process. Polym.* **2011**, *8*, 904.
- [46] U. Schnabel, M. Balazinski, R. Wagner, J. Stachowiak, D. Boehm, M. Andrasch, P. Bourke, J. Ehlbeck, *Innov. Food Sci. Emerg. Technol.* **2021**, *72*, 102745.
- [47] Z. Xu, C. Cheng, J. Shen, Y. Lan, S. Hu, W. Han, P. K. Chu, *Bioelectrochemistry* **2018**, *121*, 125.
- [48] Y.-M. Zhao, A. Patange, D.-W. Sun, B. Tiwari, *Compr. Rev. Food Sci. Food Saf.* **2020**, *19*, 3951.
- [49] H. Yu, S. Perni, J. J. Shi, D. Z. Wang, M. G. Kong, G. Shama, *J. Appl. Microbiol.* **2006**, *101*, 1323.
- [50] T. Nakajima, H. Kurita, H. Yasuda, K. Takashima, A. Mizuno, *Int. J. Plasma Environ. Sci. Technol.* **2012**, *6*, 189.
- [51] S. Nair, S. E. Finkel, *J. Bacteriol.* **2004**, *186*, 4192.
- [52] D. Pinto, M. A. Santos, L. Chambel, *Crit. Rev. Microbiol.* **2015**, *41*, 61.
- [53] M. Laroussi, *IEEE Trans. Plasma Sci.* **2002**, *30*, 1409.
- [54] M. Cooper, G. Fridman, A. Fridman, S. G. Joshi, *J. Appl. Microbiol.* **2010**, *109*, 2039.
- [55] A. Patange, D. Boehm, D. Ziuzina, P. J. Cullen, B. Gilmore, P. Bourke, *Int. J. Food Microbiol.* **2019**, *293*, 137.
- [56] E. A. J. Bartis, A. J. Knoll, P. Luan, J. Seog, G. S. Oehrlein, *Plasma Chem. Plasma Process.* **2016**, *36*, 121.
- [57] Z. Xu, J. Shen, Z. Zhang, J. Ma, R. Ma, Y. Zhao, Q. Sun, S. Qian, H. Zhang, L. Ding, C. Cheng, P. K. Chu, W. Xia, *Plasma Process. Polym.* **2015**, *12*, 827.
- [58] J. Shen, H. Zhang, Z. Xu, Z. Zhang, C. Cheng, G. Ni, Y. Lan, Y. Meng, W. Xia, P. K. Chu, *Chem. Eng. J.* **2019**, *362*, 402.
- [59] S. Khan, M. R. P. A. Rizvi, M. M. Alam, M. Rizvi, I. Naseem, *Toxicol. Rep.* **2019**, *6*, 136.
- [60] M.-L. Kung, M.-H. Tai, P.-Y. Lin, D.-C. Wu, W.-J. Wu, B.-W. Yeh, H.-S. Hung, C.-H. Kuo, Y.-W. Chen, S.-L. Hsieh, S. Hsieh, *Colloids Surf. B* **2017**, *55*, 399.
- [61] D. Bagchi, V. S. S. Rathnam, P. Lemmens, I. Banerjee, S. K. Pal, *ACS Omega* **2018**, *3*, 10877.
- [62] T. M. C. Nishime, A. C. Borges, C. Y. Koga-Ito, M. Machida, L. R. O. Hein, K. G. Kostov, *Surf. Coat. Technol.* **2017**, *312*, 19.
- [63] Y. Yang, H. Wang, H. ke, Z. Hu, W. Shang, Y. Rao, H. Peng, Y. Zheng, Q. Hu, R. Zhang, H. Luo, X. Rao, *Appl. Env. Microbiol.* **2020**, *86*, e01998.
- [64] Y. Li, J. Pan, G. Ye, Q. Zhang, J. Wang, J. Zhang, J. Fang, *Eur. J. Oral Sci.* **2017**, *125*, 463.
- [65] M. Laroussi, D. A. Mendis, M. Rosenberg, *New J. Phys.* **2003**, *5*, 41.

**How to cite this article:** A. Lavrikova, N. C. T. Dadi, H. Bujdánková, K. Hensel, *Plasma Process. Polym.* **2024**, e2300147.  
<https://doi.org/10.1002/ppap.202300147>